

# TEA<sup>+</sup>-sensitive KCNQ1 Constructs Reveal Pore-independent Access to KCNE1 in Assembled I<sub>Ks</sub> Channels

J. KUROKAWA, H.K. MOTOIKE, and R.S. KASS

From the Department of Pharmacology, College of Physicians and Surgeons of Columbia University, New York, New York 10032

**ABSTRACT** I<sub>Ks</sub>, a slowly activating delayed rectifier K<sup>+</sup> current through channels formed by the assembly of two subunits KCNQ1 (KvLQT1) and KCNE1 (minK), contributes to the control of the cardiac action potential duration. Coassembly of the two subunits is essential in producing the characteristic and physiologically critical kinetics of assembled channels, but it is not yet clear where or how these subunits interact. Previous investigations of external access to the KCNE1 protein in assembled I<sub>Ks</sub> channels relied on occlusion of the pore by extracellular application of TEA<sup>+</sup>, despite the very low TEA<sup>+</sup> sensitivity (estimated EC<sub>50</sub> > 100 mM) of channels encoded by coassembly of wild-type KCNQ1 with the wild type (WT) or a series of cysteine-mutated KCNE1 constructs. We have engineered a high affinity TEA<sup>+</sup> binding site into the h-KCNQ1 channel by either a single (V319Y) or double (K318I, V319Y) mutation, and retested it for pore-delimited access to specific sites on coassembled KCNE1 subunits. Coexpression of either KCNQ1 construct with WT KCNE1 in Chinese hamster ovary cells does not alter the TEA<sup>+</sup> sensitivity of the homomeric channels (IC<sub>50</sub> ≈ 0.4 mM [TEA<sup>+</sup>]<sub>out</sub>), providing evidence that KCNE1 coassembly does not markedly alter the structure of the outer pore of the KCNQ1 channel. Coexpression of a cysteine-substituted KCNE1 (F54C) with V319Y significantly increases the sensitivity of channels to external Cd<sup>2+</sup>, but neither the extent of nor the kinetics of the onset of (or the recovery from) Cd<sup>2+</sup> block was affected by [TEA<sup>+</sup>]<sub>o</sub> at 10× the IC<sub>50</sub> for channel block. These data strongly suggest that access of Cd<sup>2+</sup> to the cysteine-mutated site on KCNE1 is independent of pore occlusion caused by TEA<sup>+</sup> binding to the outer region of the KCNE1/V319Y pore, and that KCNE1 does not reside within the pore region of the assembled channels.

**KEY WORDS:** heart potassium channels • pore • cysteine substitution • LQT-1 • subunit assembly

## INTRODUCTION

I<sub>Ks</sub>, a slowly activating delayed rectifier K<sup>+</sup> current through channels formed by the assembly of two subunits KCNQ1 (KvLQT1) and KCNE1 (minK), contributes to the control of the duration of cardiac action potentials (Kass and Davies, 1996). The uniquely slow kinetics of I<sub>Ks</sub> are particularly well suited to time repolarization in cardiac ventricular muscle cells, where the duration of the action potential can be several hundred milliseconds (Kass, 1995, 1996; Suessbrich and Busch, 1999). KCNQ1 has six hydrophobic transmembrane segments similar to other voltage-gated K<sup>+</sup> channels, but KCNE1 is a 129-amino acid residue protein with a single transmembrane segment (Takumi et al., 1988; Barhanin et al., 1996; Sanguinetti et al., 1996) resembling β subunits of other channels (Abriel et al., 2000; Sanguinetti, 2000a). Coexpression of KCNQ1 with KCNE1 leads to slowly activating K<sup>+</sup> currents with characteristics similar to those of the native cardiac I<sub>Ks</sub> that are so crucial to the maintenance of normal cardiac function. Evidence for the importance of this current to human physiology comes from studies of the

long QT syndrome, which is an inherited arrhythmia that is correlated with episodes of syncope and sudden cardiac death (Suessbrich and Busch, 1999). Mutations that map to the *KCNQ1* and *KCNE1* genes account for >50% of reported genotyped cases of QT syndrome (Splawski et al., 1997). Some of these mutations reported in KCNE1 have been shown to modify the gating kinetics of channels expressed heterologously, suggesting that the molecular interaction between two proteins may be altered by these mutations (Splawski et al., 1997; Sesti and Goldstein, 1998). However, the molecular mechanism of the interaction between KCNQ1 and KCNE1 proteins remains to be understood.

To determine whether sites of the KCNE1 protein are exposed within the I<sub>Ks</sub> pore, Tai and Goldstein (1998) and Wang et al. (1996) performed scanning susceptibility analysis (Akabas et al., 1992; Stauffer and Karlin, 1994; Pascual et al., 1995). These experiments were carried out for I<sub>Ks</sub> channels expressed in *Xenopus* oocytes using the thiol-reactive transition metal Cd<sup>2+</sup> and a series of mutants for which a single residue was mutated to cysteine in sequential positions along the putative transmembrane segment of KCNE1. In this work, I<sub>Ks</sub> channels formed with F54C or the G55C mutant human KCNE1 were sensitive to external but not internal Cd<sup>2+</sup>, whereas those with mutation F56C were sensitive

Address correspondence to Dr. Robert S. Kass, Department of Pharmacology, College Columbia University, 630 West 168 Street, New York, NY 10032. Fax: (212) 342-2703; E-mail: rsk20@columbia.edu

to internal but not external reagent. Tai and Goldstein's hypothesis was that there is a barrier to  $\text{Cd}^{2+}$  movement between residues G55 and F56 in the conducting pore. External  $\text{Cd}^{2+}$  access to these key sites was interpreted as pore-delimited based on competition between externally applied  $\text{TEA}^+$  and  $\text{Cd}^{2+}$  in channel-blocking experiments. However, these key experiments and their interpretation were limited by the very low  $\text{TEA}^+$  sensitivity of wild-type KCNQ1 channels.

Here, we have reinvestigated pore-delimited access of the thiol-reactive reagent ( $\text{Cd}^{2+}$ ) to specific cysteine-mutated sites (F54C and G55C) on the h-KCNE1 protein by coexpressing these constructs with highly  $\text{TEA}^+$ -sensitive mutant h-KCNQ1 channels (K318I + V319Y; V319Y) in transiently transfected Chinese hamster ovary (CHO)<sup>1</sup> cells. Externally applied  $\text{TEA}^+$  rapidly, reversibly, and potentially blocked channels consisting of these mutants alone or coassembled with WT and mutant KCNE1. We tested for, but did not find evidence of, restrictions of  $\text{Cd}^{2+}$  access to F54C or G55C when this KCNE1 mutant was coexpressed with the  $\text{TEA}^+$  sensitive mutants. Our data strongly suggest that KCNE1 does not reside within the pore region and that any effects of KCNE1 assembly are likely to be due to interactions between KCNE1 and KCNQ1 that reside elsewhere, perhaps with the S4 segments themselves.

## MATERIALS AND METHODS

### Molecular Biology

The human cDNA clone *KCNQ1* was a gift from Dr. M. Keating (Department of Human Genetics, University of Utah, Salt Lake City, UT) and subcloned into the mammalian expression vector pCDNA3.1 (Invitrogen). Mutations of both KCNQ1 and KCNE1 were performed by plaque-forming unit-based mutagenesis (QuickChange™ site-directed mutagenesis kit; Stratagene), and the mutant gene fragments were inserted into translationally silent restriction sites. All sequences were performed by the chain termination method in the DNA Sequencing Facility at Columbia University. The basic protocol uses Chinese hamster ovary (CHO) cells that were cultured in Ham's F12 medium and transiently transfected using Lipofectamine with Lipofectamine-PLUS reagents (Life Technologies) as previously reported (Wang et al., 1998b). Cells were passaged the day before transfection after reaching 20–30% confluence in 25-cm<sup>2</sup> tissue culture flasks. We avoided using CHO cells after 15 passages because we found this improved our transfection efficiency and cell quality. Transfected cells were plated on small petri dishes, and cultured in an incubator with 5%  $\text{CO}_2$ .

### Electrophysiology and Data Analysis

Currents were recorded using the whole-cell patch-clamp technique (Hamill et al., 1981). CHO cells were plated in petri dishes that were placed on the stage of an inverted microscope (model IMT-2; Olympus), and the CHO medium was replaced by the Tyrode's solution before measurement of  $I_{\text{Ks}}$ . The composition of the Tyrode's solution was as follows (in mM): 132 NaCl, 4.8 KCl,

1.2  $\text{MgCl}_2$ , 2  $\text{CaCl}_2$ , 5 glucose, and 10 HEPES, pH 7.4. Membrane capacitance of the cells used in this study ranged between 8 and 25 pF. All measurements were performed at room temperature. In whole-cell patch-clamp experiments, the tip resistance of the microelectrodes (borosilicate glass capillaries) was 2–4 M $\Omega$  when filled with the following internal solution (in mM): 110 potassium aspartate, 5 ATP-K<sub>2</sub>, 11 EGTA, 10 HEPES, 1  $\text{CaCl}_2$ , and 1  $\text{MgCl}_2$ , pH 7.3. Series resistance was 3.5–8 M $\Omega$  and was electrically compensated.

Transmembrane currents were obtained using Axopatch 200A amplifiers (Axon Instruments) with 100-M $\Omega$  headstages, low-pass filtered at 2 kHz, digitized at 0.5 kHz, and sampled online to a computer hard disk. Activation (isochronal) of  $I_{\text{Ks}}$  was studied by applying 2-s depolarizing pulses in 20-mV increments from –40 mV to approximately –60 mV of holding potentials. In most of the experiments, test potentials were applied to 60 mV at 0.33 Hz. Activation was measured as the time-dependent current during test pulses or as deactivating current tails after test pulses. Most voltage protocols were designed to terminate within ~12 min to minimize rundown of the currents. pCLAMP software (version 8.0; Axon Instruments) was used both to generate the voltage-clamp protocols and to acquire data. Graphical and statistical data analysis was carried out using Origin 6.0 software (Microcal). Statistical significance was assessed with *t* test for simple comparisons: differences at  $P < 0.05$  were considered to be significant.

## RESULTS

### External $\text{TEA}^+$ Block of Wild-type and Mutant $I_{\text{Ks}}$ Channels

Because it is generally assumed that *KCNQ1* encodes the pore forming subunit of functional  $I_{\text{Ks}}$  channels (Sanguinetti et al., 1996), we sought to increase the  $\text{TEA}^+$  sensitivity of assembled  $I_{\text{Ks}}$  channels by mutating KCNQ1 as a first step in determining pore-delimited access to sites on the h-KCNE1 protein. Common residues (position 449) in the extracellular loop of the *Shaker* K<sup>+</sup> channel outer pore region have been shown to coordinate  $\text{TEA}^+$  binding (MacKinnon and Yellen, 1990) and C-type inactivation (Lopez-Barneo et al., 1993). To evaluate whether this region affects the  $\text{TEA}^+$  sensitivity of  $I_{\text{Ks}}$  channels, we mutated two residues (K318; V319) in the KCNQ1 channel according to the equivalent positions in the  $\text{Kv}_{2.1}$  channel (Lipkind et al., 1995) and KCNQ2 channel (Wang et al., 1998a), which are both sensitive to extracellular  $\text{TEA}^+$  block in the micromolar concentration range.

We next investigated the effects of these KCNQ1 mutations on gating and sensitivity to  $[\text{TEA}^+]_o$  with and without coexpression of KCNE1. In the absence of KCNE1, wild-type (WT) KCNQ1 channels were not completely blocked by >50 mM  $\text{TEA}^+$  as previously reported (Wang et al., 1996; Tai and Goldstein, 1998; Fig. 1, A and C, top), but the single mutant (V319Y) channel was reversibly blocked by 0.5 mM  $\text{TEA}^+$  (Fig. 1 B, top). At 5 mM, external  $\text{TEA}^+$  completely blocked the currents in both the double (K318I + V319Y) and the single mutant channels. Thus, the mutant KCNQ1 channels exhibit at least a 100-fold increase in the sensitivity to extracellular  $\text{TEA}^+$ . Accompanying the change in  $\text{TEA}^+$  sensitivity were mutation-induced

<sup>1</sup>Abbreviation used in this paper: CHO, Chinese hamster ovary.

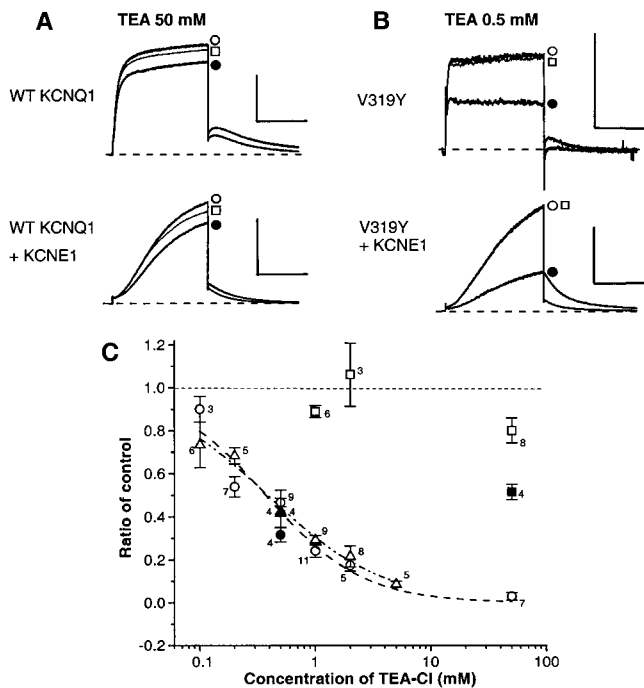


FIGURE 1. External TEA<sup>+</sup> sensitivity of K318I + V319Y and V319Y mutants of the human KCNQ1 channel in the absence and presence of KCNE1. In A and B, traces are shown for cells transfected with the indicated constructs in response to voltage pulses to +60 mV before (○) and after (●) 2-min rapid applications of extracellularly applied TEA<sup>+</sup>, and then after wash out (□). (A) The effects of 50 mM TEA<sup>+</sup> on currents measured in cells transfected with wild-type (WT) KCNQ1 with (bottom) and without (top) KCNE1. Vertical bars represent 50 pA/pF for KCNQ1 alone, 100 pA/pF KCNE1 + KCNQ1, and horizontal bars represent 1 s. (B) The effects of 0.5 mM TEA<sup>+</sup> on current recorded from cells transfected with V319Y KCNQ1 with (bottom) and without (top) KCNE1. Bars represent 5 pA/pF for KCNQ1 alone, 50 pA/pF for KCNE1 + V319Y KCNQ1 and 1 s. (C) Dose-response curves of external TEA<sup>+</sup>. Currents measured in each [TEA<sup>+</sup>] were normalized to currents in the absence of TEA<sup>+</sup> and plotted versus [TEA<sup>+</sup>]. Plotted are mean data ± SEM. The number of cells studied is indicated in parentheses. Symbols are as follows: WT KCNQ1 alone (■); WT KCNQ1 + KCNE1 (□); K318I + V319Y KCNQ1 alone (●); K318I + V319Y KCNQ1 + KCNE1 (○); V319Y KCNQ1 alone (▲); and V319Y KCNQ1 + KCNE1 (△).

changes in channel gating, which is consistent with mutation-induced inactivation of the channel (Fig. 1 B, top panel). Thus, it appears that the common residues in KCNQ1 coordinate high affinity TEA<sup>+</sup> binding and most likely C-type inactivation, as is the case in *Shaker* channels (MacKinnon and Yellen, 1990; Lopez-Barneo et al., 1993). Interestingly, coexpression with KCNE1 results in channels that activate and deactivate with kinetics remarkably similar to WT KCNQ1/KCNE1 (compare bottom panels, Fig. 1, A and B), but now also with greatly increased sensitivity to extracellular TEA<sup>+</sup> (Fig. 1 B, bottom panel). We compared the TEA<sup>+</sup> sensitivity of heteromultimeric (KCNE1/KCNQ1) and homomultimeric (KCNQ1) channels for the various KCNQ1 con-

structs in Fig. 1 C. The IC<sub>50</sub> values of TEA<sup>+</sup> block for K318I + V319Y and V319Y heteromultimeric channels (recorded at +60 mV) are 0.43 mM (nH 0.98) and 0.41 mM (nH 0.87), respectively. For both mutants, these IC<sub>50</sub> values were almost the same at +40 and +80 mV within a range between 0.4 and 0.50 mM, indicating weak voltage-dependent inhibition by TEA<sup>+</sup>, which is consistent with a TEA<sup>+</sup> binding site near the outer pore of the channel. Data for K318I + V319Y KCNQ1 channels reveal the same TEA<sup>+</sup> sensitivity in the absence or presence of KCNE1.

Mutant heteromultimeric channels retain the TEA<sup>+</sup> sensitivity of the homomultimer (Fig. 1 C), as is the case for WT KCNQ1 subunits. This result provides evidence that KCNE1 coassembly does not markedly alter the structure of the outer pore of the KCNQ1 channel. Furthermore, since we measured the same TEA<sup>+</sup> sensitivity for KCNE1 expressed with either the single or double KCNQ1 mutant, we used the V319Y KCNQ1 construct as a tool for highly TEA<sup>+</sup>-sensitive I<sub>Ks</sub> channels in the remaining experiments.

#### External Cd<sup>2+</sup> Sensitivity of WT and Cysteine-mutated KCNE1 Constructs

We next coexpressed the TEA<sup>+</sup>-sensitive KCNQ1 construct (V319Y) with the cysteine-mutated KCNE1, and determined the external Cd<sup>2+</sup> sensitivity of the KCNQ1–KCNE1 channel complex. Exposure of V319Y/WT KCNE1 channels to 2 mM Cd<sup>2+</sup> reversibly blocked the expressed current by <10% (30-s exposure). This result suggests a subtle involvement of endogenous cysteines, which causes a background block of expressed channels. We next sought to determine whether or not engineering a cysteine into KCNE1 increases the Cd<sup>2+</sup> sensitivity of the encoded channels.

We tested the Cd<sup>2+</sup> sensitivity of WT KCNQ1 coexpressed with mutant (F54C) KCNE1 (Fig. 2 B), and found the mutation significantly increased 2 mM Cd<sup>2+</sup> block approximately threefold as shown previously (Tai and Goldstein, 1998). We found a similar Cd<sup>2+</sup> sensitivity of V319Y KCNQ1/F54C and V319Y KCNQ1/G55C channels (Fig. 2, D and E) and, thus, concluded that the V319Y mutation by itself did not interfere with access of extracellularly applied Cd<sup>2+</sup> to cysteine at position 54. We also tested for, but found no evidence of, an effect of test voltage on Cd<sup>2+</sup> block of the expressed channels (data not shown), as had been reported for channels expressed in *Xenopus* oocytes (Tai and Goldstein, 1998).

Because Tai and Goldstein (1998) reported that the substitution at KCNE1 position 56 (F56C) conferred internal but not external sensitivity of expressed channels to Cd<sup>2+</sup>, we tested for similar effects in our experiments, and confirmed this observation. Coexpression of KCNQ1 with F56C KCNE1 more than doubles the sensitivity of expressed channels to internally applied 2

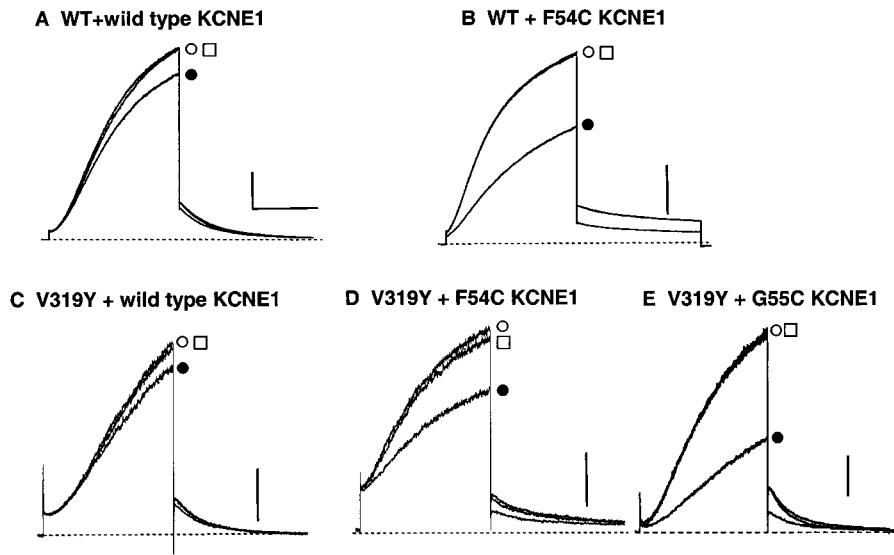


FIGURE 2. The effects of 2 mM of external  $\text{Cd}^{2+}$  on  $I_{\text{Ks}}$  channels coexpressed with wild-type or mutated (F54C) KCNE1. The figure shows typical traces recorded in response to 2-s pulses to +60 mV in the absence ( $\circ$ ) and presence ( $\bullet$ ) of 2 mM (extracellular)  $\text{Cd}^{2+}$  and then after wash out ( $\square$ ). (A) WT KCNQ1 + WT KCNE1. Bars represent 2 nA and 1 s. (B) WT KCNQ1 + F54C KCNE1. Bar: 2 nA. (C) V319Y KCNQ1 + WT KCNE1; (D) V319Y KCNQ1 + F54C KCNE1; and (E) V319Y KCNQ1 + G55C KCNE1. Bars: (C–E) 0.2 nA.

mM  $\text{Cd}^{2+}$  (percent rundown of currents for 13 min: WT  $87.7 \pm 4.2\%$ ,  $n = 5$ ; and F56C  $37.8 \pm 9.5\%$ ,  $n = 5$ ), without altering the sensitivity of the expressed channels to externally applied 2 mM  $\text{Cd}^{2+}$  (percentage of remaining currents: F56C  $90.9\%$ ,  $n = 2$ ; data not shown). Thus, our data support the view that cysteine substitution over a very short region of the KCNE1 protein (residues 54–56) confers side-specific  $\text{Cd}^{2+}$  sensitivity upon heteromultimeric KCNE1/KCNQ-1 channels. We next proceeded to use the V319Y KCNQ1 construct coexpressed with F54C and G55C KCNE1 mutants to determine whether or not external  $\text{Cd}^{2+}$  access to these sites on KCNE1 is pore-delimited.

#### Rapid Kinetics of $\text{TEA}^+$ Block

Our rapid application system (time constant  $>20$  ms) allowed us to investigate the effects of  $\text{TEA}^+$  during 2-s depolarizing pulses. As shown in Fig. 3, exposure of 10 mM  $\text{TEA}^+$  to V319Y  $I_{\text{Ks}}$  completely blocked the expressed current within 500 ms, and the block can be washed out within 200 ms. Because of the slow kinetics of the channels, both wash in and wash out could be measured during a single depolarizing pulse. The rapid and reversible block by  $\text{TEA}^+$  is consistent with interactions at the mutated site in KCNQ1 (position 319), which is equivalent to *Shaker* 449T (Yellen et al., 1991; Heginbotham and MacKinnon, 1992). Thus, our data suggest that the high affinity  $\text{TEA}^+$  block of the mutant KCNQ1 constructs is likely to occur by occluding the channel pore, and that these constructs can be used to assay pore-delimited access to sites on either channel subunit.

#### Onset of $\text{Cd}^{2+}$ Block in the Absence and Presence of $\text{TEA}^+$

Thus, we next tested for the possibility that the interaction of  $\text{Cd}^{2+}$  with the Cys at position 54 of KCNE1 is af-

ected by  $\text{TEA}^+$  block of the channels. We carried out two sets of experiments to test for this possibility. First, we measured the time course of the onset and recovery of  $\text{Cd}^{2+}$  block in the absence and presence of a saturating  $\text{TEA}^+$  concentration. If the pore of the  $I_{\text{Ks}}$  channel is occluded completely by high concentration of  $\text{TEA}^+$ , and if Cys54 was located within the pore, then we reasoned that accessibility of  $\text{Cd}^{2+}$  to Cys54 would be restricted by  $\text{TEA}^+$  block.

The protocol we chose took advantage of the application of  $\text{TEA}^+$  and  $\text{Cd}^{2+}$  via the rapid solution change system illustrated in Fig. 3 and applied in Figs. 4 and 5. For these experiments, the same concentration of  $\text{Cd}^{2+}$  application was applied in the absence or presence of  $\text{TEA}^+$  in the same cell. In the absence of  $\text{TEA}^+$ , we measured the onset of and recovery from  $\text{Cd}^{2+}$  block of the channels. In the absence of  $\text{TEA}^+$ , the application

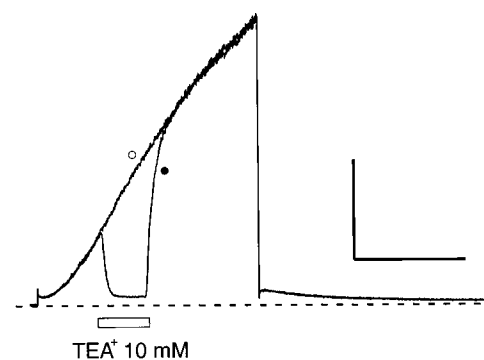


FIGURE 3. Rapid application of  $[\text{TEA}^+]_o$  (10 mM) blocks V319Y KCNQ1 + F54C KCNE1 channels. Currents were recorded by the same voltage protocol as in Fig. 2; and traces with ( $\bullet$ ) or without ( $\circ$ ) application of external  $\text{TEA}^+$  were superimposed. The duration of the rapid application of  $\text{TEA}^+$  was indicated as the white bar below the traces. Bars represent 0.5 nA and 1 s.

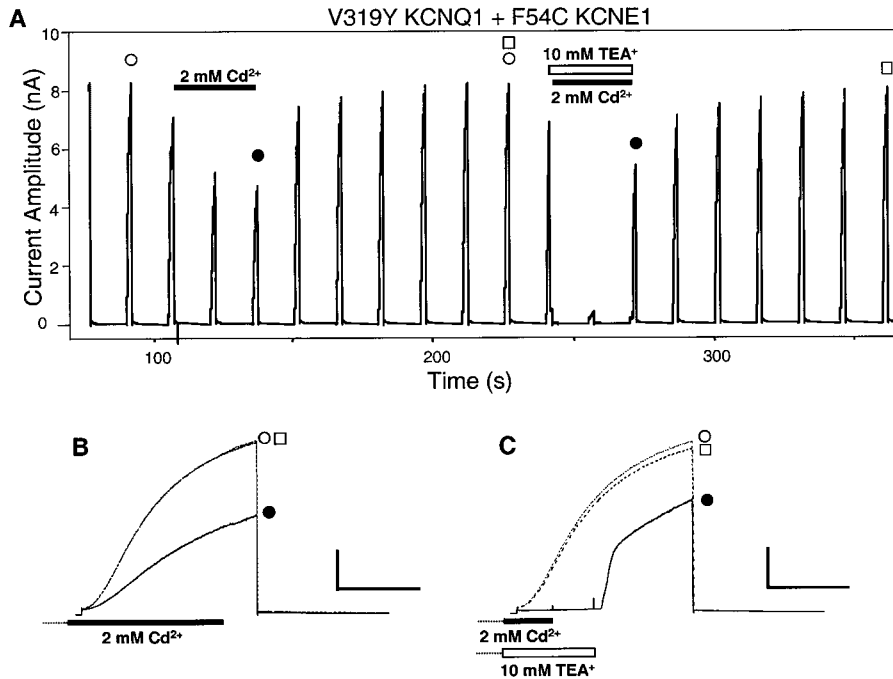


FIGURE 4. Typical recordings of the effects of external Cd<sup>2+</sup> on V319Y KCNQ1 + F54C KCNE1 channels in the absence and presence of [TEA<sup>+</sup>]<sub>o</sub> (10 mM). The currents were elicited by 2-s pulses to +60 mV every 15 s from a -60-mV holding potential. (A) The experimental procedure is shown at a slow time base. The application of Cd<sup>2+</sup> and/or TEA<sup>+</sup> is indicated as the bars above the current traces. The time scale is shown as the time after the rupture of the membrane. The traces shown in B and C are marked by an open circle (before Cd<sup>2+</sup>), closed circle (after Cd<sup>2+</sup>), and an open square (wash out). Current traces from A are displayed at a faster time base for the application of Cd<sup>2+</sup> alone (B) and for the application of Cd<sup>2+</sup> in the presence of 10 mM TEA<sup>+</sup> (C). Bars represent 2 nA and 1 s.

of Cd<sup>2+</sup> resulted in approximately a 30% reduction in the current (also see Fig. 2 D), which could be completely reversed with wash out (Fig. 4). We repeated the experiment, but in this case first applied TEA<sup>+</sup> at a sufficiently high concentration (10 mM) to completely block the channels. It was possible to assay Cd<sup>2+</sup> block of the channel that had occurred in the presence of to-

tal channel block by TEA<sup>+</sup> by quickly washing out TEA<sup>+</sup> and measuring the amplitude of the remaining current (Fig. 4, A and C). Washout of TEA<sup>+</sup> revealed Cd<sup>2+</sup>-blocked channel activity remarkably similar to that obtained in the absence of TEA<sup>+</sup> (Fig. 4, compare B and C). This and other similar experiments are summarized in Fig. 5, which confirms the observation that the magnitude Cd<sup>2+</sup> inhibition of the V319Y/F54C channel is significantly different from inhibition of V319Y/WT KCNE1 channels, but is not affected by the presence of 10 mM TEA<sup>+</sup>. These data suggest that pore occlusion by TEA<sup>+</sup> does not prevent Cd<sup>2+</sup>-access to the Cd<sup>2+</sup> sensitive site on KCNE1 (position 54).

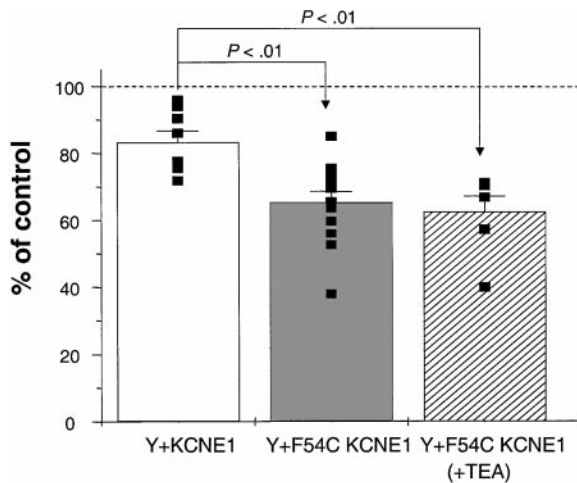


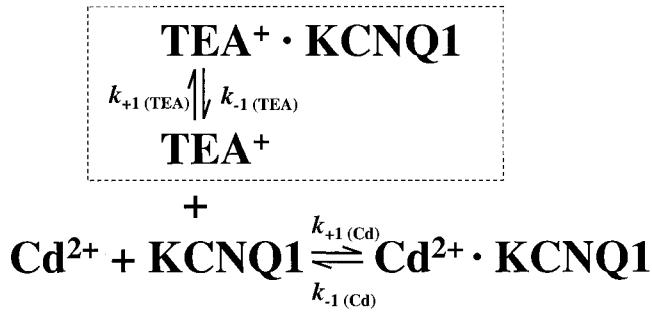
FIGURE 5. Summary of the effects of external Cd<sup>2+</sup> on TEA<sup>+</sup>-sensitive constructs. The percentage of remaining current after a 30-s application of 2 mM Cd<sup>2+</sup> was normalized to current before Cd<sup>2+</sup> application. The currents were elicited by the same voltage protocol as that in Fig. 4. White column shows block of V319Y KCNQ1 + WT KCNE1 constructs without TEA<sup>+</sup> ( $n = 8$ ). Gray column shows block of V319Y KCNQ1 + F54C KCNE1 constructs without TEA<sup>+</sup> ( $n = 12$ ). Hatched column shows block for V319Y KCNQ1 + F54C KCNE1 constructs in the presence of 10 mM TEA<sup>+</sup> outside ( $n = 6$ ) measuring the data according to Fig. 4 A.

#### Influence of TEA<sup>+</sup> on the Kinetics of Cd<sup>2+</sup> Block

Binding of TEA<sup>+</sup> and Cd<sup>2+</sup> to their respective sites of interaction is a dynamic process and possible effects of TEA<sup>+</sup> on Cd<sup>2+</sup> binding will be determined by the on and off rates of the two ions. Assuming pore-limited access of Cd<sup>2+</sup> to the F54C KCNE1 site, a simple model for Cd<sup>2+</sup> binding is shown in Scheme 1. In the simplest case, because of rapid TEA<sup>+</sup> kinetics, TEA<sup>+</sup> is in equilibrium (within dotted square in Scheme 1), and Cd<sup>2+</sup> is assumed to bind only to the fraction of channels that are not blocked by TEA<sup>+</sup> ( $f_{UB}$ ). This fraction of channels is defined as:

$$f_{UB} = [\text{TEA}]_o / ([\text{TEA}]_o + k_{-1(\text{TEA})} / k_{+1(\text{TEA})}), \quad (1)$$

where  $k_{+1(\text{TEA})}$  and  $k_{-1(\text{TEA})}$  represent the apparent onset rate constant ( $\text{s}^{-1}\text{M}^{-1}$ ) and the apparent off rate constant for TEA<sup>+</sup> ( $\text{s}^{-1}$ ), respectively. The kinetics of



SCHEME 1.

$\text{Cd}^{2+}$  block of the channel can be calculated by considering the interaction of  $\text{Cd}^{2+}$  with channels that are not blocked by  $\text{TEA}^+$ , or  $f_{\text{UB}}$  derived above. The equation for the time constant ( $\tau$ ) of  $\text{Cd}^{2+}$  block (unblock) of channels in the presence of  $\text{TEA}^+$  will be:

$$1/\tau = (f_{\text{UB}} \cdot L \cdot k_1 + k_{-1}), \quad \text{or} \quad (2)$$

$$\tau = (f_{\text{UB}} \cdot L \cdot k_1 + k_{-1})^{-1}, \quad (3)$$

where  $\tau$  is the time constant in seconds,  $L$  is the concentration of  $\text{Cd}^{2+}$  in moles,  $k_1$  is the apparent onset rate constant ( $\text{s}^{-1}\text{M}^{-1}$ ), and  $k_{-1}$  is the apparent off rate constant for  $\text{Cd}^{2+}$  ( $\text{s}^{-1}$ ). To test this prediction, experimental determination of the parameters in Eq. 3 is needed. The data in Fig. 1 can be used to estimate  $f_{\text{UB}}$  as a function of  $[\text{TEA}]_o$ , but the rate constants  $k_{-1}$  and  $k_1$  must be extracted from kinetic data for  $\text{Cd}^{2+}$  block.

We first estimated the association rate constant for  $\text{Cd}^{2+}$  inhibition of  $I_{\text{Ks}}$  assuming that the onset of  $\text{Cd}^{2+}$ -induced inhibition also obeyed pseudo-first order association kinetics. Fig. 6 A shows a typical recording for  $\text{Cd}^{2+}$  block of V319Y/F54C currents and a plot of the averaged peak currents versus time of application of  $\text{Cd}^{2+}$ . The onset of block was well fit by a single-exponential decay function. On average, the onset time constant was  $12.5 \pm 2.2$  s ( $n = 4$ ) and, thus, the association rate ( $k_{\text{app}}$ ) was  $\sim 0.08$   $\text{s}^{-1}$ . We next determined  $k_{-1}$  from the wash out of  $\text{Cd}^{2+}$  block in Fig. 6 B. As in the experiment of Fig. 4, we first exposed the cell to  $\text{Cd}^{2+}$ , blocked the channels, and returned it to  $\text{Cd}^{2+}$ -free solution. After washing out  $\text{Cd}^{2+}$ , the currents recovered slowly to the control values with averaged time constant of  $20.1 \pm 1.1$  s ( $n = 4$ ). Assuming pseudo-first order dissociation kinetics, the dissociation rate constant ( $k_{-1}$ ) is  $0.05$   $\text{s}^{-1}$ . Thus, the association rate constant ( $k_1 = (k_{\text{app}} - k_{-1})/L$ ) and the apparent dissociation constant ( $K_d = k_{-1}/k_1$ ) were estimated  $15$   $\text{M}^{-1}\text{s}^{-1}$  and  $3.3 \times 10^{-3}$  M, respectively.

We next began testing for evidence of overlap of  $\text{TEA}^+$  and  $\text{Cd}^{2+}$  binding sites in the channels by studying the influence of externally applied  $\text{TEA}^+$  on the kinetics of  $\text{Cd}^{2+}$  block of expressed channels. As shown in the bottom panels of Fig. 6, we found no significant effect of external  $\text{TEA}^+$  (2 mM) on the onset or recovery from  $\text{Cd}^{2+}$  block of V319Y/F54C channels (onset  $\tau = 16.4 \pm 2.8$  s [ $P = 0.06$  versus control; paired  $t$  test]; and offset  $\tau = 21.5 \pm 0.9$  s [ $P = 0.25$  versus control; paired  $t$  test]). These data suggest that the sites for  $\text{TEA}^+$  and  $\text{Cd}^{2+}$  block do not overlap. We repeated these experiments testing for the effects of extracellu-

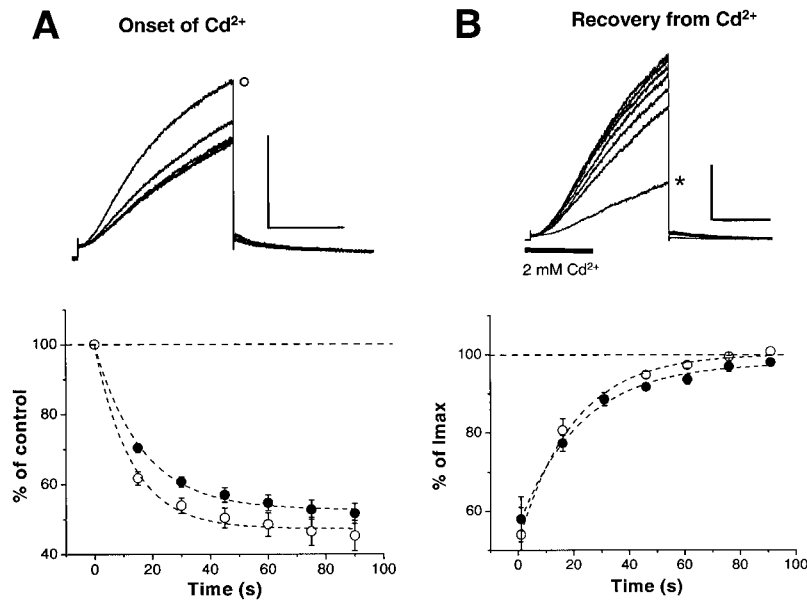


FIGURE 6. Kinetics of  $\text{Cd}^{2+}$  block of V319Y KCNQ1 + F54C KCNE1 channels. Currents were measured by the same voltage protocol as that in Fig. 4. (A) Onset of block. Superimposed traces (top) recorded before ( $\circ$ ) and once every 15 s after the application of  $\text{Cd}^{2+}$  (2 mM). Bars represent 0.5 nA and 1 s. The bottom panel shows averaged plot of currents measured at the end of each depolarizing voltage pulse normalized to control, pre- $\text{Cd}^{2+}$  current, plotted versus time after  $\text{Cd}^{2+}$  application in the absence ( $\circ$ ) and presence ( $\bullet$ ) of 2 mM  $\text{TEA}^+$ . The dashed curves are the best fit single-exponential function to the data ( $\tau = 12.8$  s [ $\circ$ ] and  $16.4$  s [ $\bullet$ ]). (B) Recovery from  $\text{Cd}^{2+}$  block. The top panel shows current block measured every 15 s after washing out  $\text{Cd}^{2+}$  (2 mM) as indicated by solid bar in the figure. The trace marked by the asterisk is the first measured after washing out  $\text{Cd}^{2+}$ . Bars represent 0.4 nA and 1 s. The bottom panel shows the averaged plot of currents normalized end of pulse current versus time after wash out of  $\text{Cd}^{2+}$  in the absence ( $\circ$ ) and presence ( $\bullet$ ) of 2 mM  $\text{TEA}^+$ , and the dashed curves are the best fit single-exponential function ( $\tau = 19.8$  s [ $\circ$ ] and  $22.6$  s [ $\bullet$ ]) to the data.

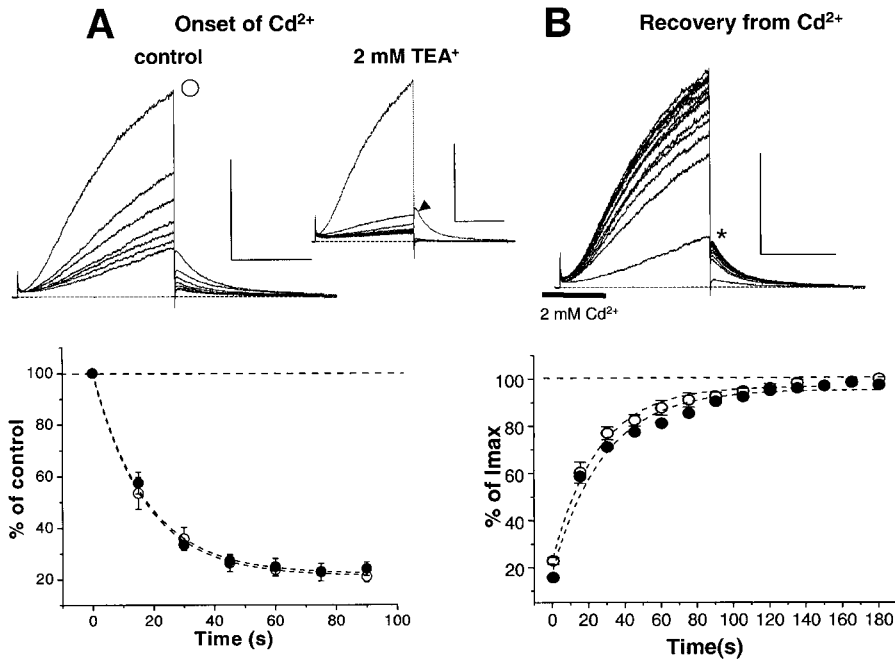


FIGURE 7. Kinetics of  $\text{Cd}^{2+}$  block of V319Y KCNQ1 + G55C KCNE1 channels. The experimental protocol and format of the plots are same as that in Fig. 6. (A) Onset of  $\text{Cd}^{2+}$  (2 mM) block. Superimposed traces (top) recorded before ( $\circ$ ) and once every 15 s after the  $\text{Cd}^{2+}$  application. In the presence of 2 mM  $\text{TEA}^+$ , the trace before the  $\text{Cd}^{2+}$  application is marked by an arrowhead. Bars represent 0.5 nA and 1 s. In the bottom panel, the dashed curves are the best fit single-exponential function to the data ( $\tau = 17.2$  s [ $\circ$ , control], 17.3 s [ $\bullet$ , 2 mM  $\text{TEA}^+$ ]). (B) Recovery from 2 mM  $\text{Cd}^{2+}$  block. Bars for superimposed traces represent 0.5 nA and 1 s. In the bottom panel, the dashed curves are the best fit single-exponential function to the data ( $\tau = 25.2$  s [ $\circ$ , control], 28.1 s [ $\bullet$ , 2 mM  $\text{TEA}^+$ ]).

lar  $\text{TEA}^+$  on  $\text{Cd}^{2+}$  block of a second KCNE1 mutant (G55C), in which the mutated cysteine may be located deeper within the channel pore and, thus, more susceptible to occlusion by  $\text{TEA}^+$  block of the channel. However, as was the case for V391Y/F54C channels, we found no effect of  $\text{TEA}^+$  on the on or off kinetics of  $\text{Cd}^{2+}$  block of V319Y/G55C channels (Fig. 7).

Finally, to test the predictions of the effects of  $\text{TEA}^+$  on the kinetics of  $\text{Cd}^{2+}$  block more completely, we investigated the effects of a broad range of  $\text{TEA}^+$  concentrations on  $\text{Cd}^{2+}$  block. We measured the ratio of time constants of  $\text{Cd}^{2+}$  block in the presence ( $\tau$ ) and absence ( $\tau_0$ ) of  $\text{TEA}^+$ , which according to Eqs. 1–3, is given by the following relationship:

$$\tau/\tau_0 = (L + K_d)/(f_{UB} \cdot L + K_d), \quad (4)$$

where terms are as defined above. In the limit when  $f_{UB} = 0$ , or when all channels are blocked by  $\text{TEA}^+$ , this reduces to  $\tau/\tau_0 = (L/K_d + 1)$ .

The results of our experiments are summarized in Fig. 8. First, we confirmed that, at 10 mM [ $\text{Cd}^{2+}$ ] $_o$ , expression of V319Y KCNQ1 and F54C KCNE1 encodes  $\text{Cd}^{2+}$ -sensitive channels. We have found that a 30-s application of 10 mM  $\text{Cd}^{2+}$  suppressed the currents by  $70.1 \pm 3.9\%$  ( $n = 5$ ), compared with  $26.0 \pm 9.6\%$  ( $n = 3$ ) suppression of V319Y/WT channels, indicating significant  $\text{Cd}^{2+}$  block conferred by the F54C mutation. Next, we determined the kinetics of the onset of  $\text{Cd}^{2+}$  block in the presence and absence of  $\text{TEA}^+$  and the experiments are summarized in Fig. 8. Fig. 8 (A and B) illustrates records and summary data from a typical ex-

periment in which we measured the effects of 2 mM  $\text{TEA}^+$  on  $\text{Cd}^{2+}$  block of the channels. In the same cell, we first applied 10 mM  $\text{Cd}^{2+}$  for a fixed period (1.5 min; Fig. 8 A), and measured the effects of the cation on currents (asterisks) recorded during depolarizing pulses (Fig. 8 B). We washed out  $\text{Cd}^{2+}$  (closed circle), applied 2 mM  $\text{TEA}^+$  which blocked the currents by 80% ( $f_{UB} = 0.20$ ) (arrowhead), and reapplied 10 mM  $\text{Cd}^{2+}$  (asterisks in Fig. 8 B, top). On average (five cells), we found the  $f_{UB}$  value was  $0.18 \pm 0.01$ . We then used this value and calculated the  $\tau/\tau_0$  ratio in each cell. At 2 mM  $\text{TEA}^+$ , we determined a mean  $\tau/\tau_0$  ratio of  $1.1 \pm 0.1$ , which is much smaller than the ratio of 2.6 predicted by Eq. 4 using our measured dissociation constant (3.3 mM). Other  $\tau/\tau_0$  ratios were determined with different concentrations of  $\text{TEA}^+$ , and then summarized in Fig. 8 D. For comparison, we repeated these experiments for KCNQ1 (WT)/F54C channels over a much higher range of  $\text{TEA}^+$  concentrations (Fig. 1). We found that neither 50 mM  $\text{TEA}^+$  ( $f_{UB} = 0.71$ ) nor 100 mM  $\text{TEA}^+$  ( $f_{UB} = 0.3$ ) markedly affects the kinetics of  $\text{Cd}^{2+}$  block of expressed channels in contrast to the results of similar experiments in *Xenopus* oocytes (Tai and Goldstein, 1998). The simplest interpretation of these results is that  $\text{TEA}^+$ -induced pore occlusion does not limit the access of externally applied  $\text{Cd}^{2+}$  to KCNE1 residues, Cys54 and 55 on the KCNE1–KCNQ1 channel complex expressed in CHO cells.

#### DISCUSSION

We have used the substitute cysteine accessibility method (Karlin and Akabas, 1998) to reinvestigate the

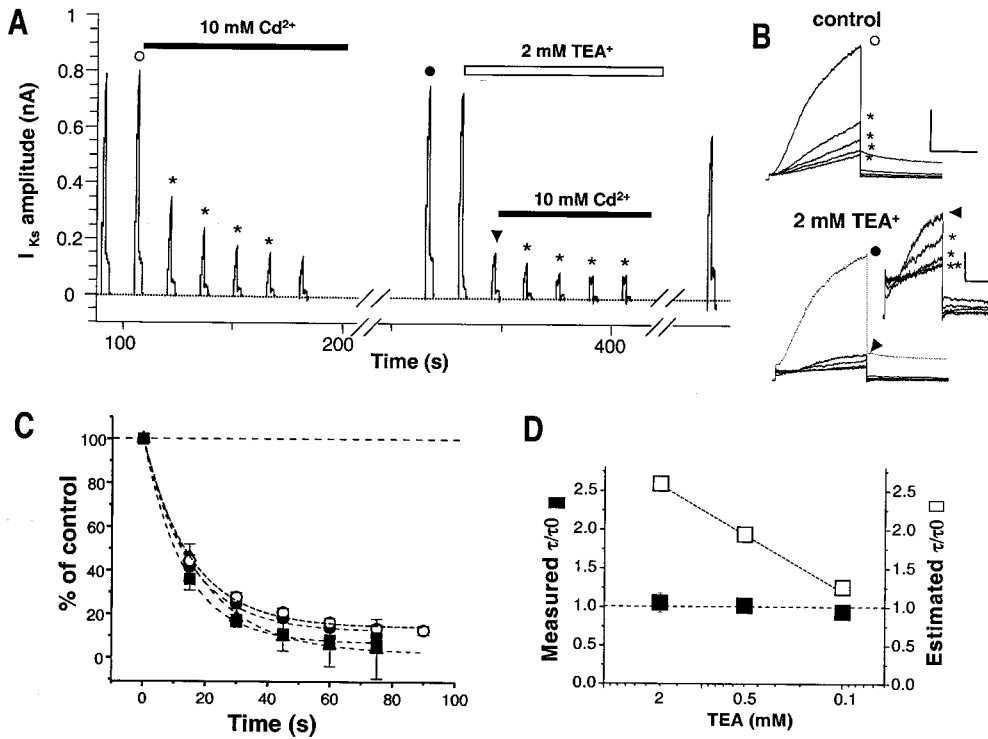


FIGURE 8. TEA<sup>+</sup> does not alter the kinetics of Cd<sup>2+</sup> (10 mM) block of V319Y KCNQ1 + F54C KCNE1 channels. (A) Currents are shown recorded at a slow time base illustrating the onset of Cd<sup>2+</sup> block of channel activity in the absence (left) and presence (right) of TEA<sup>+</sup> (2 mM). The application of the test compounds is illustrated as bars above the current traces, which were recorded continuously in the same cell. The time scale indicates the time after the rupture of the membrane to establish whole-cell recording conditions, and the broken axis reflects the period in which Cd<sup>2+</sup> was washed out after the first exposure. (B) Superposition of current traces recorded every 30 s during the onset of Cd<sup>2+</sup> block. Symbols or asterisks in A mark the traces that are shown in B. Bars represent 0.25 nA and 1 s. In the inset

of right panel, the traces in the presence of TEA<sup>+</sup> are plotted at higher gain as indicated by the same arrows. In this case, the bars represent 50 pA and 1 s. (C) Averaged plots are shown in the same format in Fig. 6 A in the absence (○,  $\tau = 15.4$  s) and presence of TEA at 0.1 mM (■,  $\tau = 13.2$  s) and 0.5 mM (●,  $\tau = 14.6$  s) and 2 mM (▲,  $\tau = 17.8$  s). (D) Plotted are the expected (□) and measured (■) ratios of time constant of Cd<sup>2+</sup> (10 mM) block in presence ( $\tau$ ) and absence ( $\tau_0$ ) of TEA<sup>+</sup> (0.1 mM;  $n = 3$ , 0.5 mM;  $n = 3$ , 2 mM;  $n = 5$ ). In each case,  $f_{UB}$  (the fraction of unbound channels) was measured. The estimated ratio  $\tau/\tau_0$  was determined using the mean  $f_{UB}$  value (0.182) and Eq. 4.

location of the KCNE1 subunit relative to the outer pore of assembled  $I_{Ks}$  channels. This methodology, in which reporter cysteines are engineered into specific regions of interest in channel proteins, was used in this study to test the influence of externally applied TEA<sup>+</sup> upon access of the thiol-reactive reagent Cd<sup>2+</sup> to cysteine-substituted residues on KCNE1 that previously had been suggested to line the pore of assembled  $I_{Ks}$  channels (Tai and Goldstein, 1998). In the present experiments, we expressed cysteine-substituted KCNE1 mutants with a KCNQ1 construct that also had been mutated to encode highly TEA<sup>+</sup>-sensitive channels. Together, these constructs, expressed in CHO cells, provided a system in which we could investigate side-specific effects of Cd<sup>2+</sup> on expressed channel activity, and determine whether or not external application of TEA<sup>+</sup> over a low concentration range altered these interactions. Our results indicate that, as previously reported (Tai and Goldstein, 1998), the distinction between external and internal access to reporter cysteines was detected over a very small range of KCNE1 residues (Tai and Goldstein, 1998). However, in contrast to previous studies, we find that access of externally applied Cd<sup>2+</sup> to KCNE1 residue C54 was not prevented by TEA<sup>+</sup> pore occlusion. These results clearly show that

access of Cd<sup>2+</sup> to the cysteine-substituted KCNE1 residue is independent of the pore occlusion by external TEA<sup>+</sup>, and argue against the possibility that KCNE1 lines the pore of assembled  $I_{Ks}$  channels.

#### Consideration of Previous Data

Our results contradict the interpretation of previous experimental previous data, obtained primarily in *Xenopus* oocytes, which suggested that the same cysteine-substituted site (F54C, KCNE1) is exposed deep into the conducting pore (Tai and Goldstein, 1998). How may the two sets of data be reconciled? First, we confirm that intracellularly applied Cd<sup>2+</sup> does not access site Cys54, but it does interact with the cysteine-mutated residue at position 56. Hence, as was shown in previous experiments by Tai and Goldstein (1998), there is a very narrow region over which the KCNE1 protein apparently is exposed to intracellular and extracellular water-filled pathways. However, neither the kinetics nor the magnitude of the Cd<sup>2+</sup> block of cysteine-substituted F56C subunits expressed with V319Y KCNQ1 subunits was affected by externally applied TEA<sup>+</sup>, arguing against pore-delimited access to of Cd<sup>2+</sup> to this site. Both K318I + V319Y and V319Y channels were reversibly blocked by, and with, the same sensitivity to exter-



nal TEA<sup>+</sup> regardless of coassembly with KCNE1, indicating that KCNE1 coassembly does not markedly alter the structure of the outer pore of KCNQ1 channel. This contrasts with WT KCNQ1 channels, which were not completely blocked by >50 mM TEA<sup>+</sup> in the absence or presence of KCNE1.

#### *Association with KCNE1 Protein Does Not Markedly Alter the Structure of the Outer Pore of KCNQ1 Channel*

In the present experiments, because we studied channels expressed in CHO cells in which endogenous expression of KCNQ1 subunits is minimal (Barhanin et al., 1996; Sanguinetti et al., 1996), we were able to focus on activity of channels encoded by mutant constructs of both key subunits. In addition, comparison between the effects of Cd<sup>2+</sup> block of channels assembled by mutant and wild-type KCNE1 were used to exclude the influence of 13 endogenous cysteine residues in KCNQ1 and cysteine at position 106 in KCNE1 in the effects we investigated. Furthermore, we were careful to limit the concentration range of Cd<sup>2+</sup> in experiments designed to inhibit channel activity to minimize other known effects of Cd<sup>2+</sup> on I<sub>Ks</sub> channel activity such as changes in surface potential (Kwok and Kass, 1993; Daleau et al., 1997; Wickenden et al., 1999).

#### *Implications for KCNE1/KCNQ1 Assembly*

How is it possible to reconcile our data with previous investigations of the location of KCNE1 relative to the KCNQ1 channel pore? In terms of structure and molecular size, it is unlikely that KCNE1 lines the deep pore in the vicinity of the K<sup>+</sup> channel selectivity filter (Doyle et al., 1998). However, recent experiments in which the crystal structure of the CSA potassium channel have been analyzed in the absence (Doyle et al., 1998) and presence of subunit coassembly (Gulbis et al., 2000) indicate that a complex structural architecture that can exist in the regions of interactions between protein subunits (raising the possibility of alternate geometries) may explain these data. In case of voltage-gated Na<sup>+</sup> channels, the S4 voltage-sensing region has shown to move inside a narrow cavity that is distinct from the ion conducting pore (Yang et al., 1996). Furthermore, in *Shaker* K<sup>+</sup> channels, the possibility of extra pore crevices has been recently suggested to explain local changes in ionic strength on channel gating (Islas and Sigworth, 2000). It is possible, should similar crevices exist for the KCNE1–KCNQ1 channel complex, that KCNE1 may link intra- and extra-space across a narrow portion of the crevice.

#### *Implications for Other Channels*

KCNE1 is the first member of a family of proteins referred to as KCNE proteins. Coassembly of KCNE1 with KCNQ1 causes marked changes in channel gating

and single-channel properties (Barhanin et al., 1996; Romey et al., 1997; Splawski et al., 1997; Sesti and Goldstein, 1998; Tristani-Firouzi and Sanguinetti, 1998; Yang and Sigworth, 1998), and KCNE1 can coassemble with HERG channels and alter their properties (McDonald et al., 1997). Modulation of channel gating by other members of both the KCNQ and KCNE gene families has been demonstrated with equally impressive functional changes in the properties of the expressed channels (Abbott and Goldstein, 1998; Abbott et al., 1999; Schroeder et al., 2000) and multiple mutations in members of each gene family have been linked to human disease (Sanguinetti, 2000b). Our data suggest that the interactions between these two families of subunits do not occur entirely within the pore region of the encoded channels, but instead suggest interaction of regions with other regions, perhaps with S4 segments themselves.

We thank Dr. J. Pascual for discussion and helpful suggestions with this work.

This work is supported by U.S. Public Health Service Grant HL 44365-5 (to R.S. Kass) and Uehara Memorial Foundation, Japan (to J. Kurokawa).

*Submitted: 2 August 2000*

*Revised: 20 October 2000*

*Accepted: 21 October 2000*

#### REFERENCES

- Abbott, G.W., and S.A. Goldstein. 1998. A superfamily of small potassium channel subunits: form and function of the MinK-related peptides (MiRPs). *Q. Rev. Biophys.* 31:357–398.
- Abbott, G.W., F. Sesti, I. Splawski, M.E. Buck, M.H. Lehmann, K.W. Timothy, M.T. Keating, and S.A. Goldstein. 1999. MiRP1 forms IKr potassium channels with HERG and is associated with cardiac arrhythmia. *Cell.* 97:175–187.
- Abriel, H., H. Motoike, and R.S. Kass. 2000. KChAP: a novel chaperone for specific K<sup>+</sup> channels key to repolarization of the cardiac action potential. Focus on “KChAP as a chaperone for specific K<sup>+</sup> channels”. *Am. J. Physiol. Cell Physiol.* 278:C863–C864.
- Akabas, M.H., D.A. Stauffer, M. Xu, and A. Karlin. 1992. Acetylcholine receptor channel structure probed in cysteine-substitution mutants. *Science.* 258:307–310.
- Barhanin, J., F. Lesage, E. Guillemare, M. Fink, M. Lazdunski, and G. Romey. 1996. K<sub>v</sub>LQT1 and IsK (minK) proteins associate to form the I<sub>Ks</sub> cardiac potassium current. *Nature.* 384:78–80.
- Daleau, P., M. Khalifa, and J. Turgeon. 1997. Effects of cadmium and nisoldipine on the delayed rectifier potassium current in guinea pig ventricular myocytes. *J. Pharmacol. Exp. Ther.* 281:826–833.
- Doyle, D.A., J.M. Cabral, R.A. Pfuetzner, A. Kuo, J.M. Gulbis, S.L. Cohen, B.T. Chait, and R. MacKinnon. 1998. The structure of the potassium channel: molecular basis of K<sup>+</sup> conduction and selectivity. *Science.* 280:69–77.
- Gulbis, J.M., M. Zhou, S. Mann, and R. MacKinnon. 2000. Structure of the cytoplasmic beta subunit-T1 assembly of voltage-dependent K<sup>+</sup> channels. *Science.* 289:123–127.
- Hamill, O.P., A. Marty, E. Neher, B. Sakmann, and F.J. Sigworth. 1981. Improved patch-clamp techniques for high-resolution current recording from cells and cell-free membrane patches. *Pflügers Arch.* 391:85–100.
- Heginbotham, L., and R. MacKinnon. 1992. The aromatic binding

- site for tetraethylammonium ion on potassium channels. *Neuron*. 8:483–491.
- Islas, L.D., and F.J. Sigworth. 2000. The influence of a gating pore on charge movement in  $K^+$  channels. *Biophys. J.* 78:7. (Abstr.)
- Karlin, A., and M.H. Akabas. 1998. Substituted-cysteine accessibility method. *Methods Enzymol.* 293:123–145.
- Kass, R.S. 1995. Ionic basis of electrical activity in the heart. In *Physiology and Pathophysiology of the Heart*. N. Sperelakis, editor. Kluwer Academic, Norwell, MA. 77–90.
- Kass, R.S. 1996. Delayed potassium channels in the heart: regulatory and molecular properties. In *Molecular Physiology and Pharmacology of Cardiac Ion Channels and Transporters*. M. Morad, S. Ebashi, W. Trautwein, and Y. Kurachi, editors. Kluwer Academic Publishers, Boston. 169–176.
- Kass, R.S., and M.P. Davies. 1996. The roles of ion channels in an inherited heart disease: molecular genetics of the long QT syndrome. *Cardiovasc. Res.* 32:443–454.
- Kwok, W.M., and R.S. Kass. 1993. Block of cardiac ATP-sensitive  $K^+$  channels by external divalent cations is modulated by intracellular ATP. Evidence for allosteric regulation of the channel protein. *J. Gen. Physiol.* 102:693–712.
- Lipkind, G.M., D.A. Hanck, and H.A. Fozzard. 1995. A structural motif for the voltage-gated potassium channel pore. *Proc. Natl. Acad. Sci. USA.* 92:9215–9219.
- Lopez-Barneo, J., T. Hoshi, S.H. Heinemann, and R.W. Aldrich. 1993. Effects of external cations and mutations in the pore region on C-type inactivation of *Shaker* potassium channels. *Recept. Channels.* 1:61–71.
- MacKinnon, R., and G. Yellen. 1990. Mutations affecting TEA blockade and ion permeation in voltage-activated  $K^+$  channels. *Science.* 250:276–279.
- McDonald, T.V., Z. Yu, Z. Ming, E. Palma, M.B. Meyers, K.W. Wang, S.A. Goldstein, and G.I. Fishman. 1997. A minK-HERG complex regulates the cardiac potassium current  $I_{Kr}$ . *Nature.* 388:289–292.
- Pascual, J.M., C.C. Shieh, G.E. Kirsch, and A.M. Brown. 1995.  $K^+$  pore structure revealed by reporter cysteines at inner and outer surfaces. *Neuron.* 14:1055–1063.
- Romey, G., B. Attali, C. Chouabe, I. Abitbol, E. Guillemare, J. Barhanin, and M. Lazdunski. 1997. Molecular mechanism and functional significance of the MinK control of the KvLQT1 channel activity. *J. Biol. Chem.* 272:16713–16716.
- Sanguinetti, M.C. 2000a. Maximal function of minimal  $K^+$  channel subunits. *Trends Pharmacol. Sci.* 21:199–201.
- Sanguinetti, M.C. 2000b. Long QT syndrome: ionic basis and arrhythmia mechanism in long QT syndrome type 1. *J. Cardiovasc. Electrophysiol.* 11:710–712.
- Sanguinetti, M.C., M.E. Curran, A. Zou, J. Shen, P.S. Spector, D.L. Atkinson, and M.T. Keating. 1996. Coassembly of  $K_vLQT1$  and minK (IsK) proteins to form cardiac  $I_{Ks}$  potassium channel. *Nature.* 384:80–83.
- Schroeder, B.C., S. Waldegger, S. Fehr, M. Bleich, R. Warth, R. Greger, and T.J. Jentsch. 2000. A constitutively open potassium channel formed by KCNQ1 and KCNE3. *Nature.* 403:196–199.
- Sesti, F., and S.A. Goldstein. 1998. Single-channel characteristics of wild-type  $I_{Ks}$  channels and channels formed with two minK mutants that cause long QT syndrome. *J. Gen. Physiol.* 112:651–663.
- Splawski, I., M. Tristani-Firouzi, M.H. Lehmann, M.C. Sanguinetti, and M.T. Keating. 1997. Mutations in the hminK gene cause long QT syndrome and suppress  $I_{Ks}$  function. *Nat. Genet.* 17:338–340.
- Stauffer, D.A., and A. Karlin. 1994. Electrostatic potential of the acetylcholine binding sites in the nicotinic receptor probed by reactions of binding-site cysteines with charged methanethiosulfonates. *Biochemistry.* 33:6840–6849.
- Suessbrich, H., and A.E. Busch. 1999. The  $I_{Ks}$  channel: coassembly of IsK (minK) and KvLQT1 proteins. *Rev. Physiol. Biochem. Pharmacol.* 137:191–226.
- Tai, K.K., and S.A. Goldstein. 1998. The conduction pore of a cardiac potassium channel. *Nature.* 391:605–608.
- Takumi, T., H. Ohkubo, and S. Nakanishi. 1988. Cloning of a membrane protein that induces a slow voltage-gated potassium current. *Science.* 242:1042–1045.
- Tristani-Firouzi, M., and M.C. Sanguinetti. 1998. Voltage-dependent inactivation of the human  $K^+$  channel KvLQT1 is eliminated by association with minimal  $K^+$  channel (minK) subunits. *J. Physiol.* 510:37–45.
- Wang, K.W., K.K. Tai, and S.A. Goldstein. 1996. MinK residues line a potassium channel pore. *Neuron.* 16:571–577.
- Wang, H.S., Z. Pan, W. Shi, B.S. Brown, R.S. Wymore, I.S. Cohen, J.E. Dixon, and D. McKinnon. 1998a. KCNQ2 and KCNQ3 potassium channel subunits: molecular correlates of the M-channel. *Science.* 282:1890–1893.
- Wang, W., J. Xia, and R.S. Kass. 1998b. MinK-KvLQT1 fusion proteins, evidence for multiple stoichiometries of the assembled IsK channel. *J. Biol. Chem.* 273:34069–34074.
- Wickenden, A.D., R.G. Tsushima, V.A. Losito, R. Kaprielian, and P.H. Backx. 1999. Effect of  $Cd^{2+}$  on Kv4.2 and Kv1.4 expressed in *Xenopus* oocytes and on the transient outward currents in rat and rabbit ventricular myocytes. *Cell Physiol Biochem.* 9:11–28.
- Yang, N., A.L. George, Jr., and R. Horn. 1996. Molecular basis of charge movement in voltage-gated sodium channels. *Neuron.* 16:113–122.
- Yang, Y., and F.J. Sigworth. 1998. Single-channel properties of  $I_{Ks}$  potassium channels. *J. Gen. Physiol.* 112:665–678.
- Yellen, G., M.E. Jurman, T. Abramson, and R. MacKinnon. 1991. Mutations affecting internal TEA blockade identify the probable pore-forming region of a  $K^+$  channel. *Science.* 251:939–942.